Magazine of Concrete Research
Volume 63 Issue 4

Progressive collapse-resisting capacity of RC beam–column sub-assemblage
Choi and Kim

Magazine of Concrete Research, 2011, **63**(4), 297–310
doi: 10.1680/macr.9.00170
Paper 900170
Received 15/09/2009; revised 29/05/2010; accepted 16/06/2010
Published online ahead of print 09/03/2011

ice
Institution of Civil Engineers
publishing

Progressive collapse-resisting capacity of RC beam–column sub-assemblage

H. Choi
Research engineer, Research Institute of Technology, Samsung Engineering & Construction, Seoul, Korea

J. Kim
Professor, Department of Architectural Engineering, Sungkyunkwan University, Suwon, Korea

Experiments were carried out to investigate the progressive collapse-resisting capacity of reinforced concrete beam–column sub-assemblages designed with and without seismic load. The two-span sub-assemblages were designed as part of five- and eight-storey reinforced concrete moment-resisting frames. The exterior columns of the right-hand girders were designed to be 1·5 times larger in size than the middle columns to take into account continuation of the girder. A monotonically increasing load was applied at the middle column of the specimens and force–displacement relationships were plotted. It was observed that the non-seismically designed specimen failed by crushing of concrete at the exterior column–girder joint of the left-hand girder before catenary action was activated. However, the force–displacement relationship of the specimen designed for seismic load kept increasing after fracture of the girder lower rebars near the middle column due to the catenary force of the upper rebars. Based on the test results it was concluded that significant catenary action of girders could be induced in reinforced concrete moment-resisting buildings designed as per current seismic design codes against progressive collapse initiated by sudden loss of a column.

Introduction

From a series of accidents it was observed that, in order to prevent progressive collapse, a structure should have continuity for offering an alternate path and stability of the structure when an element of vertical load-resisting systems is removed. Eurocode 1 (CEN, 2002) presented a design standard for selecting plan types for preventing progressive collapse and recommended that buildings should be integrated. In the USA, the American Concrete Institute (ACI, 2005) requires structural integrity (e.g. continuity insurance of reinforcing bars) so that partial damage by abnormal load does not result in total collapse. The American Society of Civil Engineers (ASCE, 2005) recommends a design method and load combination as well as structural integrity. The General Service Administration (GSA, 2003) presented practical design guidelines to reduce the collapse potential of federal buildings and the Department of Defense (DoD, 2005) also presented a guideline for new and existing DoD buildings. Ellingwood (2006) summarised strategies for progressive collapse risk mitigation and identified the challenges for implementing general provisions in the design codes. Starossek (2007) suggested that progressive collapse produced by various mechanisms can be classified into five distinct types: pancake, zipper, domino, section and instability. Much research has been conducted on the collapse behaviour of moment-resisting frames caused by a sudden loss of columns (Khandelwal and El-Tawil, 2005; Kim and Kim, 2009, Kim *et al.*, 2009a; Tsai and Lin 2008).

Recently, the effect of catenary action on progressive collapse has been investigated. Kim and An (2009) investigated the effect of catenary action on the progressive collapse potential of steel structures. Milner *et al.* (2007) and Sasani and Kropelnicki (2008) carried out experiments to study the behaviour of a scaled model of a continuous perimeter beam in a reinforced concrete (RC) frame structure following removal of a supporting column. Yi *et al.* (2008) carried out a static experimental study of a three-storey RC frame structure to investigate progressive failure due to the loss of a lower storey column. In those experiments it was observed that, after the plastic mechanism formed, the concrete strain in the compression zone at the beam ends reached its ultimate compressive strain and the compressive rebars were gradually subject to tension with increasing displacement. Finally, at large deformation, catenary action was activated in floor beams due to the tensile resistance of the reinforcing bars.

Previous experimental research on RC beam–column sub-assemblages has been carried out under the assumption or experimental condition that longitudinal rebars are continuous in both sides of the spans from which a column is removed. In this study, monotonic tests of RC beam–column sub-assemblages designed with and without seismic load were carried out to investigate the progressive collapse-resisting capacity. The two-span sub-assemblages were designed as part of five- and eight-storey RC moment-resisting frames. Based on the test results, the performance of an eight-storey RC moment frame with a missing column was evaluated by pushdown analysis and the results were compared with those obtained by using the member limit state recommended in FEMA-356 (FEMA, 2000).

Catenary action in progressive collapse

Generally, large deformations of beams are involved in the process of progressive collapse caused by sudden removal of a column; the geometric and material non-linearities need to be included in the analysis modelling. Figure 1 depicts the deformation of a beam–column subsystem subjected to small and large deformations caused by loss of the centre column. Under small deformation the beams are subjected mainly to bending and no axial force is induced in the cross-section (Figure 1(a)). However, as vertical deformation increases, the neutral axis moves upward and the unbalanced force below and above the neutral axis produces axial force. Finally, both tensile and compressive rebars are subjected to tension and the beams start to act like suspended cables (Figure 1(b)). This is referred to as catenary action of beams. The catenary force, however, can be activated only when the beam–column connections are strong enough to resist the catenary force of the beams. Figure 2 shows the progressive collapse-resisting capacity and variation of member forces of a steel beam–column sub-assemblage depending on whether catenary action is considered or not in the analysis modelling. The span length L is 6 m and the beams are made of H $300 \times 175 \times 7{\cdot}5 \times 10$ mm. It can be observed that when catenary action is not considered, the bending moment keeps increasing and no axial force is induced in the beams. However, when

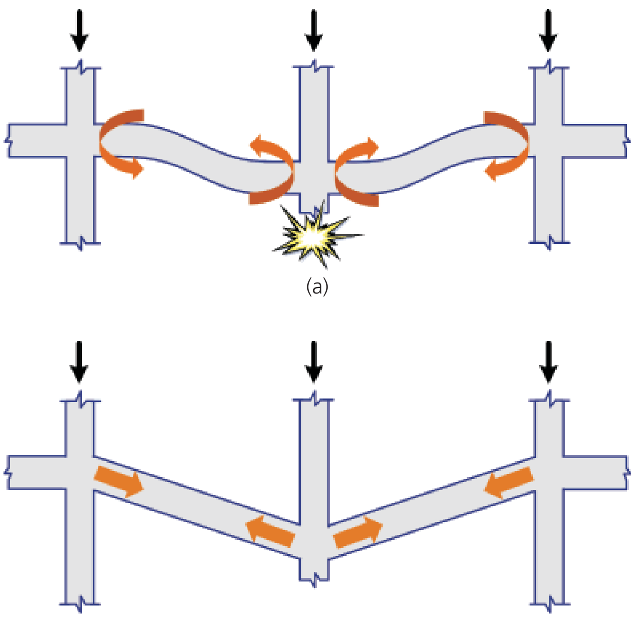

Figure 1. Deformation modes of beams depending on vertical displacement: (a) bending deformation of beams at small vertical displacement; (b) catenary action of beams at large vertical displacement

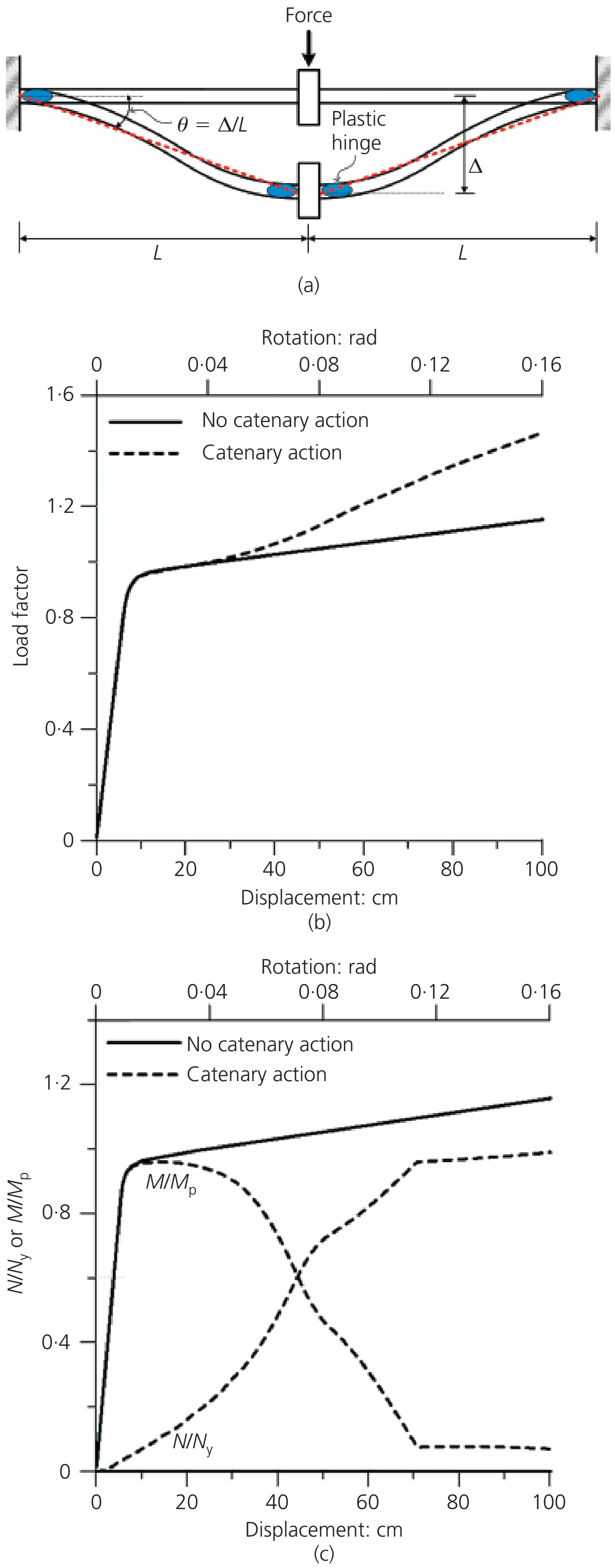

Figure 2. Pushdown analysis results of the beam–column sub-assemblage: (a) analysis model; (b) load–displacement relationship; (c) variation of member forces (N, axial force; N_y, axial force at yield; M, bending moment; M_p, plastic moment)

catenary action is considered, the bending moment decreases after flexural yielding and the axial force increases until tensile yielding. Activation of catenary action in beams may help provide an alternate load path in the case of progressive failure.

From analysis of RC moment frames it was observed that the number of rebars – both longitudinal and transverse – is the most important factor for early initiation of catenary action and for achievement of high strength (Kim and Yu, 2011). In the analysis it was assumed that the beam–column connections had sufficient strength to resist the catenary force induced in the beams. In practice, however, only a finite length of reinforcing steel is embedded in the connections, especially in the exterior connections, and it is not known whether the bond strength is sufficient for activation of catenary action. The amount of longitudinal steel and stirrups depends significantly on the design load considered, as do the activation of catenary force and its effect on progressive collapse-resisting capacity.

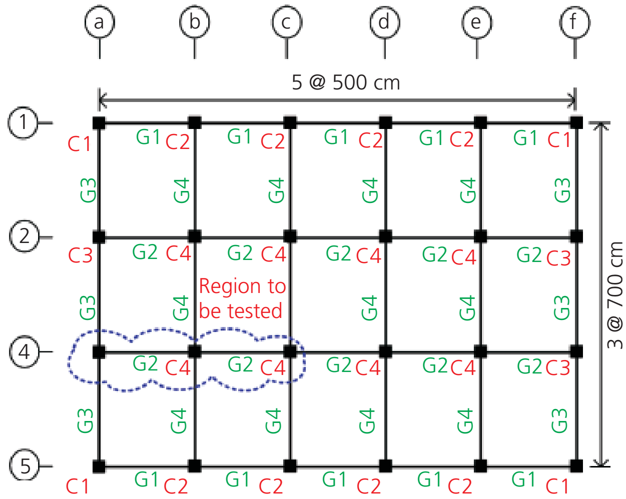

Figure 3. Plan layout of the prototype structures: C represents column and G represents girder

Experimental programme

Design of model structures and testing specimens

It has been reported that damage to the Alfred P. Murrah building as a result of a bomb attack would have been significantly reduced if the structure had been seismically designed (Ellingwood *et al.*, 2007). In the current work, five- and eight-storey RC prototype structures were designed in accordance with ACI 318-05 (ACI, 2005), with and without considering seismic load. The storey heights of the model structures were 3·5 m, and the design dead and live loads were 5·9 and 2·45 kN/m^2, respectively. The design spectral response acceleration parameters for seismic load, S_{DS} and S_{D1}, were 0·44 and 0·23, respectively (in International Building Code (ICC, 2006) format); the response modification factor R was 5·0. A design compressive strength of concrete (f'_c) of 21 was used for the five-storey structure and 30 MPa for the eight-storey structure. The yield strength of rebars was $F_y = 392$ MPa.

To evaluate the progressive collapse-resisting capacity of a beam–column sub-assemblage, scaled models of the part enclosed in the dotted curve in Figure 3 were manufactured for testing. To compare the performance of the sub-assemblage depending on concrete strength and amount and detailing of rebars, four different specimens were constructed. The seismic and non-seismic designed specimens of the five-storey structure were named 5S and 5G, respectively, and those of the eight-storey structure 8S and 8G, respectively. The detail design of the specimens was conducted based on the ACI detailing manual (ACI, 2004). The scales of the specimens corresponding to the sub-assemblages of the five- and eight-storey structures were 37 and 35%, determined in consideration of the capacity of the testing facility. Member sizes and rebar placements are shown in Tables 1–4, and details of the rebar placements of specimens 8G and 8S are depicted in Figure 4. The right-hand columns in the test specimens were made 1·5 times larger than the left-hand columns, considering the fact that girder rebars were continuous through the internal columns. In the case of non-seismically designed beams, bottom bars extended into the support (the exterior column) without a hook. However, the top and bottom bars of the seismically designed specimens were anchored with a standard 90° hook into the exterior columns. To take into account the continuation of the right-hand girder (G2 in Figure 3) in the specimens, the longitudinal bars were anchored with the tail extension of the hook. The length of the tail of the hook was longer than that required in the code (ACI, 2004). D10 (nominal diameter 9·53 mm) rebars were used for the main reinforcing steel for beams and columns, and Ø6 steel bars were used for stirrups and tie bars. From coupon tests of rebars used in the specimens, it was observed that the yield and ultimate strengths of the main rebars were 493 and 611 MPa, respectively, and those of the stirrups and tie bars 363 and 423 MPa, respectively. It was assumed that the five-storey structure was an old structure with its concrete strength somewhat deteriorated. Specimens 5S and 5G were therefore cast with concrete with a higher water/cement ratio; the concrete strength was determined to be 17 MPa from cylinder tests. The concrete strength of specimens 8S and 8G was 30 MPa.

Test set-up

Figure 5 shows the test set-up for the specimens. The right- and left-hand columns were fixed to the jigs and the actuator was connected to the middle column. It was assumed that the middle columns of the sub-assemblages were removed by accident and displacement-controlled monotonic pushdown force was applied at the middle column using a hydraulic actuator with a maximum capacity of 2000 kN and maximum stroke of ±250 mm. The tests were carried out horizontally; to prevent vertical deflection of the specimens due to self-weight, rollers were placed beneath the beam–column joint during the test as shown in Figure 6. Strain

Member		Column		Beam (G2) (depth × width)		
		Exterior (C3)	Interior (C4)			
Prototype frame	Size: mm	450 × 450	500 × 500		600 × 400	
	Rebar	4 D25	8 D25	Top	3 D25*	2 D25†
					2 D25	
				Bottom	2 D25	3 D25
Specimen	Size: mm	170 × 170	185 × 185		225 × 150	
	Rebar	4 D10	8 D10	Top	3 D10	2 D10
					2 D10	
				Bottom	2 D10	3 D10

*Longitudinal reinforcement at both ends of beam
†Longitudinal reinforcement at middle of beam

Table 1. Sectional properties of region tested in model 5S (five-storey, seismic-load-resisting)

Member		Column		Beam (G2) (depth × width)		
		Exterior (C3)	Interior (C4)			
Prototype frame	Size: mm	450 × 450	450 × 450		500 × 400	
	Rebar	4 D25	8 D25	Top	2 D25	2 D25
				Bottom	2 D25	2 D25
Specimen	Size: mm	170 × 170	170 × 170		185 × 150	
	Rebar	4 D10	8 D10	Top	2 D10	2 D10
				Bottom	2 D10	2 D10

Table 2. Sectional properties of region tested in model 5G (five-storey, gravity-load-resisting)

Member		Column		Beam (G2) (depth × width)		
		Exterior (C3)	Interior (C4)			
Prototype frame	Size: mm	500 × 500	550 × 550		550 × 400	
	Rebar	6 D25	12 D25	Top	3 D25*	2 D25†
					2 D25	
				Bottom	3 D25	3 D25
Specimen	Size: mm	180 × 180	190 × 190		195 × 140	
	Rebar	6 D10	12 D10	Top	3 D10	2 D10
					2 D10	
				Bottom	3 D10	3 D10

*Longitudinal reinforcement at both ends of beam
†Longitudinal reinforcement at middle of beam

Table 3. Sectional properties of region tested in model 8S (eight-storey, seismic-load-resisting frame)

Member		Column			Beam (G2) (depth × width)	
		Exterior (C3)	Interior (C4)			
Prototype frame	Size: mm	450 × 450	550 × 550		450 × 350	
	Rebar	4 D25	8 D25	Top	2 D25	2 D25
				Bottom	2 D25	2 D25
Specimen	Size: mm	160 × 160	190 × 190		160 × 125	
	Rebar	4 D10	8 D10	Top	2 D10	2 D10
				Bottom	2 D10	2 D10

Table 4. Sectional properties of region tested in model 8G (eight-storey, gravity-load-resisting frame)

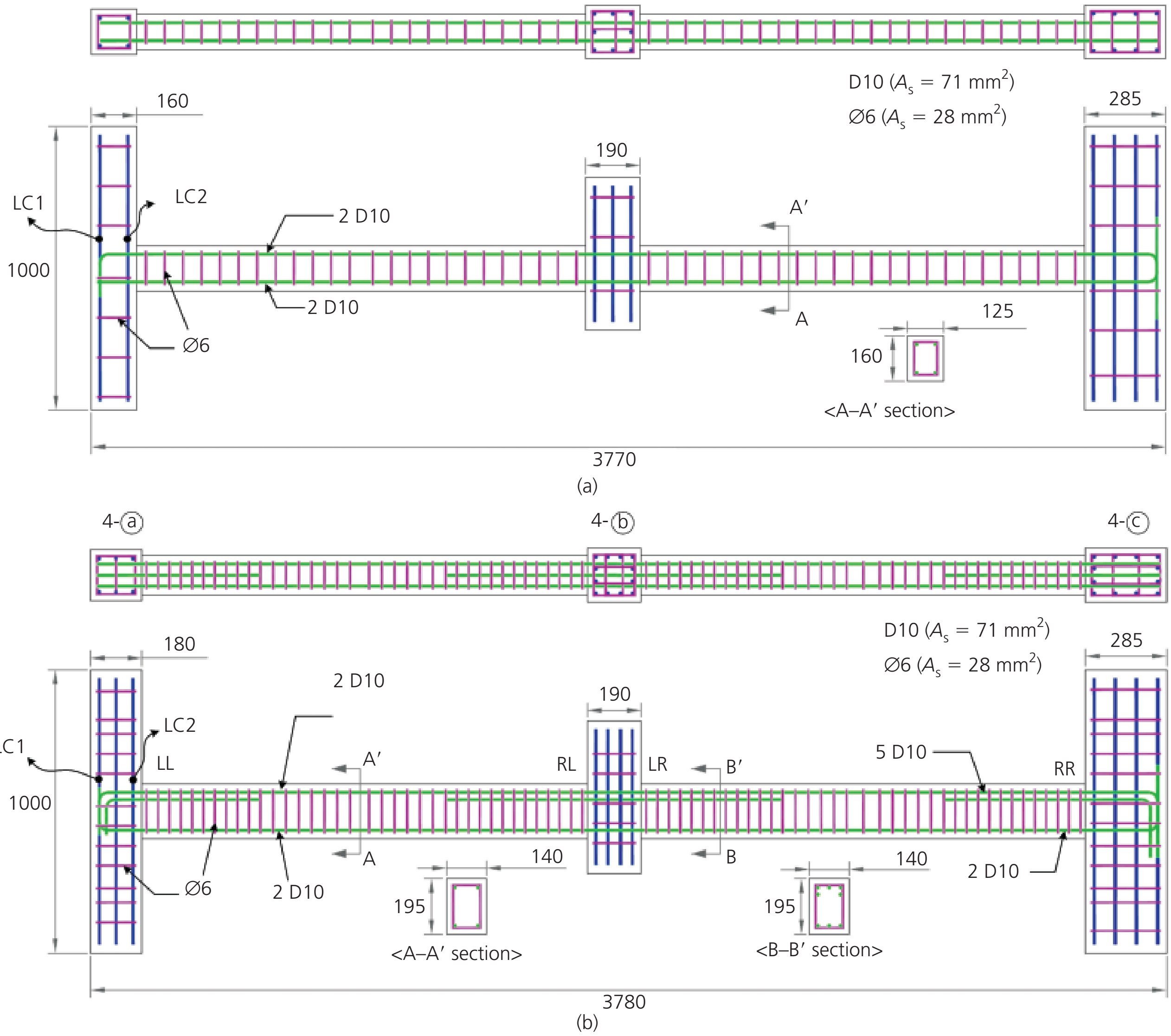

Figure 4. Reinforcement detailing of the sub-assemblage specimens (eight-storey structure): (a) gravity-load-resisting frame (8G); (b) seismic load-resisting frame (8S). Dimensions in mm; A_s is the cross-sectional area of steel bar

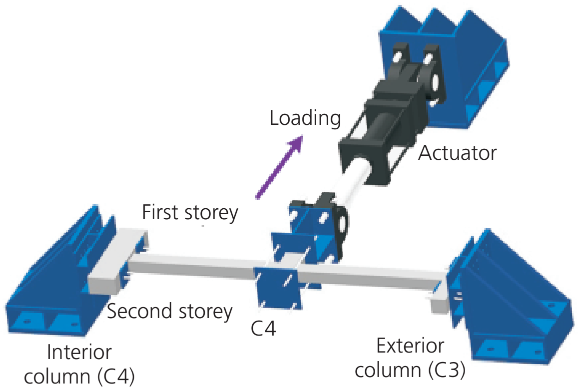

Figure 5. Test set-up for the beam–column sub-assemblage specimens

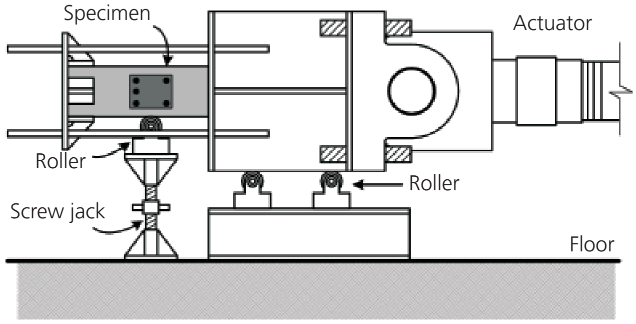

Figure 6. Supporting structure of the specimens

gauges were attached on the longitudinal rebars located at the ends of girders and at columns.

Experimental results

Failure modes of test specimens

Figure 7 shows the deformed shape and crack pattern of specimens 8S and 8G. In specimen 8G (part of the eight-storey gravity-load-resisting system), plastic hinges formed at the ends of the girders accompanied by flexural cracks and crushing of concrete under compression. As deflection increased, major cracks formed at the exterior beam–column connection, which led to connection failure (Figure 7(a)). It was also observed that, at failure, most damage was concentrated at the ends of the beams. In specimen 8S (which is part of the seismic-load-resisting system), it was noted that, after plastic hinges formed at both ends of the beams, damage spread towards the centre of the beams (Figure 7(b)). This is due to the enhanced amount of shear reinforcement at the ends of the beams and the seismic detailing of the rebars at the beam–column joints including anchoring of bottom rebars using standard hooks. The cracks formed in the middle of the beams perpendicular to the beam axis seemed to be results of catenary action of the beams at large vertical displacement. Figures 8 and 9 show the damage in the beam–exterior-column joints at failure of the sub-assemblages. The damage states of both 5G and 5S, made of concrete with a compressive strength of 17 MPa, are similar to that of specimen 8G. This implies that concrete strength is an important factor in preventing splitting of the concrete in a beam–column joint and distributing damage along the beams. That is, to activate catenary action of beams, the beam–column joint, especially the exterior joints, should retain concrete strength sufficient to resist the tensile force generated in the hooks of the longitudinal bars even in seismic-load-resisting systems. In specimen 8G, the beam longitudinal steels (which were embedded in the joints without hooks) were pulled out from the joints at joint failure (Figure 9(a)). It was only in specimen 8S – designed with seismic detailing and with a concrete compressive strength of 30 MPa – that major damage occurred at beam ends, not at the joints, and cracks were distributed throughout the beams.

Force–displacement relationships

Figure 10 shows the load–displacement relationships of the sub-assemblage specimens. It can be observed that the maximum strengths of the sub-assemblages designed for seismic load are almost twice as high as those of the specimens not designed for seismic load. The strength of the specimens dropped rapidly when the bottom rebars, which were subjected to tension, fractured. The strength of specimen 8G, however, soon recovered and kept increasing as catenary force of the beams contributed from the top rebars was activated. At small deformation, the top rebars were subjected mostly to compression; however, at large deformation both top and bottom rebars were under tensile catenary force and resisted collapse of the specimen. The catenary forces of the other specimens could not be activated since the concrete of the beam–column joints fail to provide proper anchorage for the rebars. Based on the experimental results, it can be concluded that RC moment frames that are seismically designed using a concrete strength high enough to provide strong anchorage for beam rebars can resist progressive collapse by activation of beam catenary force.

In the experiments of Sasani and Kropelnicki (2008) and Yi *et al.* (2008), which were carried out with interior girder–column sub-assemblages, damage was observed only in the girders, not in the girder–column joints. However, in this study of girder–column sub-assemblages it was observed that the concrete strength and anchoring detailing of rebars in an exterior joint played important roles in activating catenary action of girders.

Strain of longitudinal rebars

Figure 11 shows normal strain of the rebars in specimen 8S, which shows that the strain of all the rebars subjected to tensile force reached 0·003 (the yield strain obtained from the coupon test) at a vertical displacement of around or a little less than 50 mm. This corresponds well with the force–displacement relationship of specimen 8S depicted in Figure 10(b), in which the system yielded at a vertical displacement of about 50 mm.

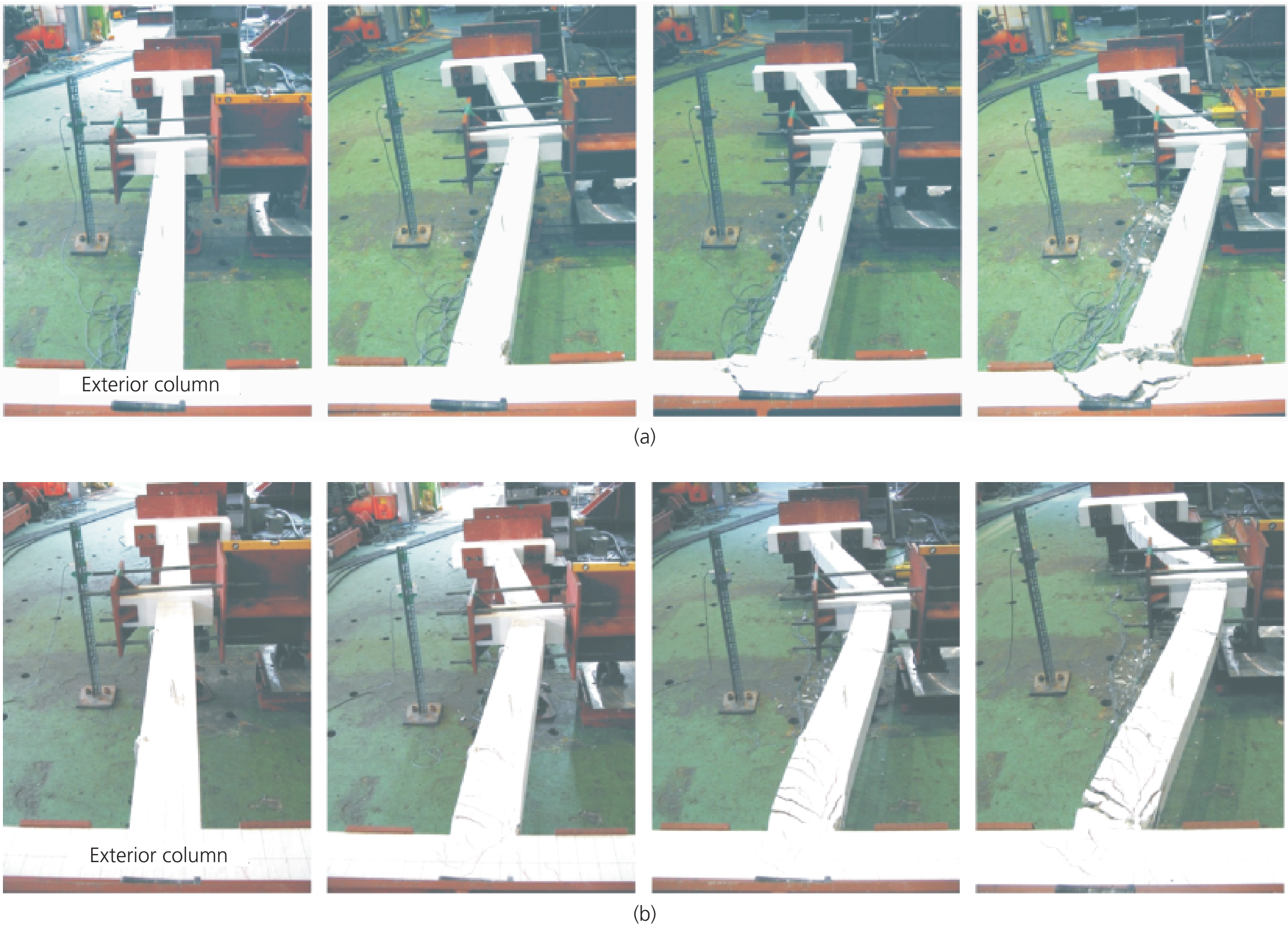

Figure 7. Deformation configurations of the specimens at various loading steps (sub-assemblage from the eight-storey structure): (a) 8G; (b) 8S

The specimen showed ductile behaviour until the vertical displacement reached about 250 mm. The force then increased again until the strength suddenly dropped at a displacement of 363 mm due to fracture of the bottom rebars in the right-hand girder. Figure 11 shows that when the vertical displacement exceeded 250 mm, the strain of the compressive rebars started to decrease. In particular, the bottom bars located in the left end of the left-hand beam were subjected to tension when the vertical displacement exceeded 315 mm.

The pushdown curve of specimen 8G, shown in Figure 10(b), increased again at a vertical displacement of about 200 mm and started to decrease as the displacement exceeded about 250 mm. The strain–displacement relationship of the specimen 8G presented in Figure 12 shows that the strain of the rebars under compression (the left-end bottom bars of left-hand beam (LL, Figure 12(a)), the right-end top bars of the left-hand beam (RL, Figure 12(b)) and the left-end top bars of the right-hand beam (LR, Figure 12(c))) generally decreased after vertical displacement of about 200 mm was reached. The strain then decreased to zero and started to be subjected to tension. As vertical displacement increases, however, the stress is reversed again and the rebars located in RL and LR are subjected to compression. The variation of rebar force seems to be due to the formation of cracks, especially in the exterior beam–column joint. Figure 12(a) shows that the rebars located in the LL of specimen 8G are subjected to compression (bottom bars) or to slight tension (bottom bars) when vertical displacement exceeds 300 mm. This implies that catenary force is not activated in the beam of the specimen designed only for gravity load, even at large deformation. A similar phenomenon can be observed in specimen 5S, as shown in Figure 13(a) in which all rebars are under compression at large deformation. Figures 13(b) and 13(c) also show that the strains of the top rebars of specimen 5S located at RL and LR decrease at vertical displacements of 263 and 285 mm, respectively. These displacements correspond to the points of rapid drop

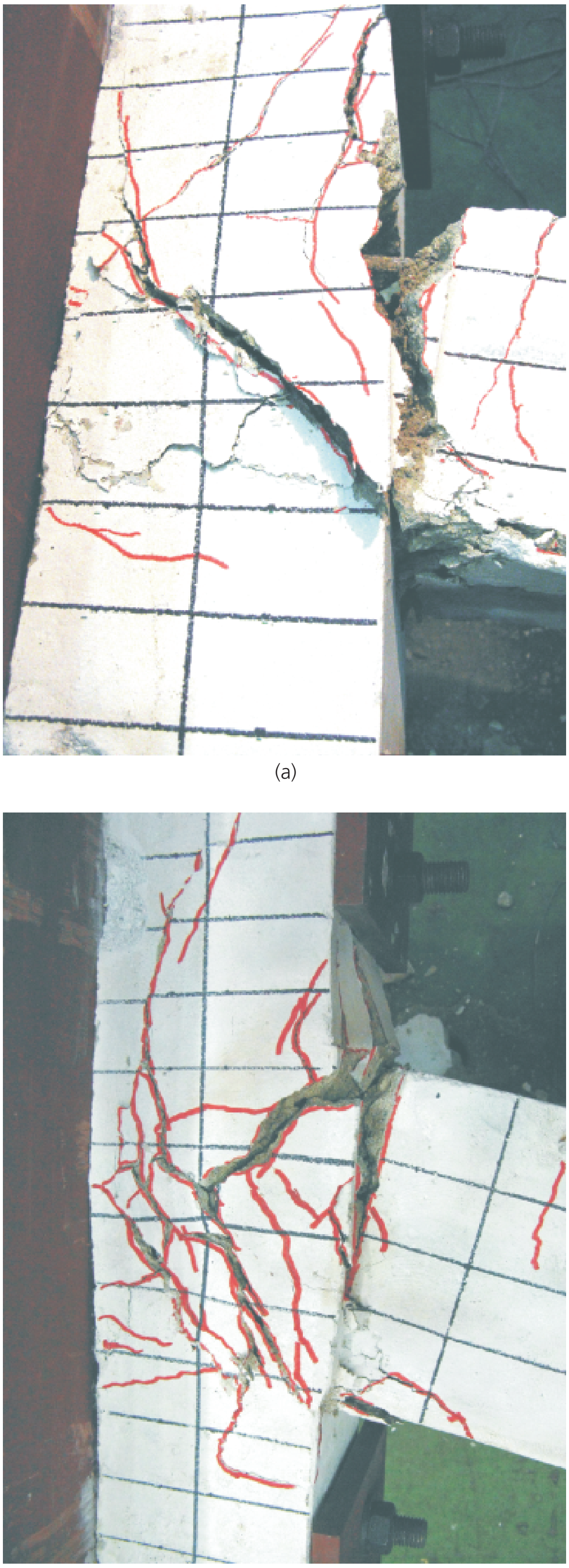

(a)

(b)

Figure 8. Damaged beam–column joints of the sub-assemblage from the five-storey structure: (a) 5G; (b) 5S

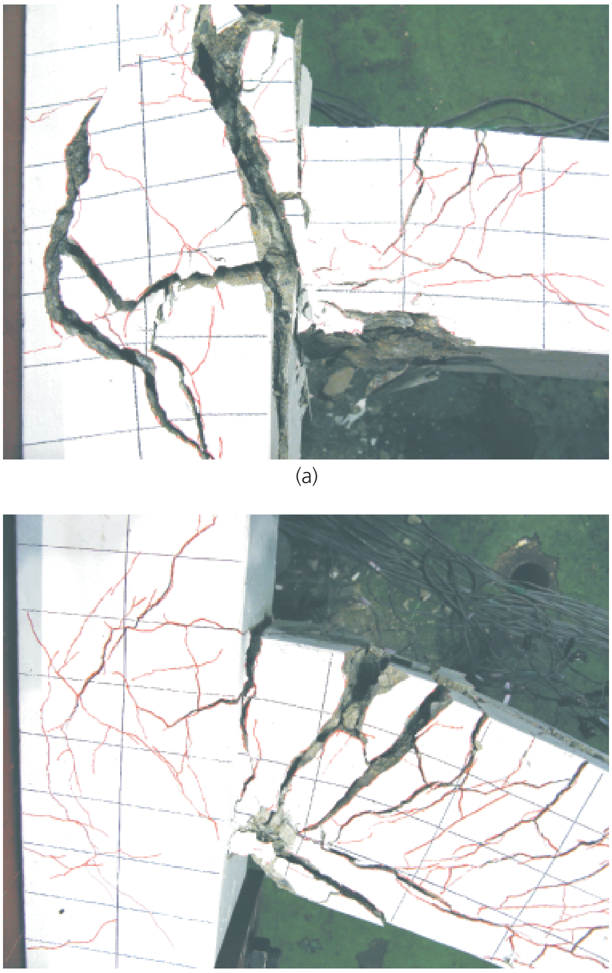

(a)

(b)

Figure 9. Damaged beam–column joints of the sub-assemblage from the eight-storey structure: (a) 8G; (b) 8S

of force, as can be observed in the force–displacement relationship depicted in Figure 10(a).

Figure 14 shows the axial strains of the exterior main rebar (LC1) and the interior main rebar (LC2) of the exterior columns in specimens 8G and 8S (the locations of the rebars LC1 and LC2 are depicted in Figure 4). It can be observed that the exterior rebar of model 8G, which was subjected to compression at first, started to resist tension at a vertical displacement of about 130 mm. However, the main rebar LC2 of model 8S started to be subjected to tension at the larger displacement of about 200 mm, due mainly to the more closely spaced tie bars. The interior rebar LC2 in specimen 8S was also subjected to larger tension from the first stage of loading.

Progressive collapse potential of eight-storey model structure

In this section, progressive collapse potential of the frame of the eight-storey structure shown in Figure 3 (labelled ④) was

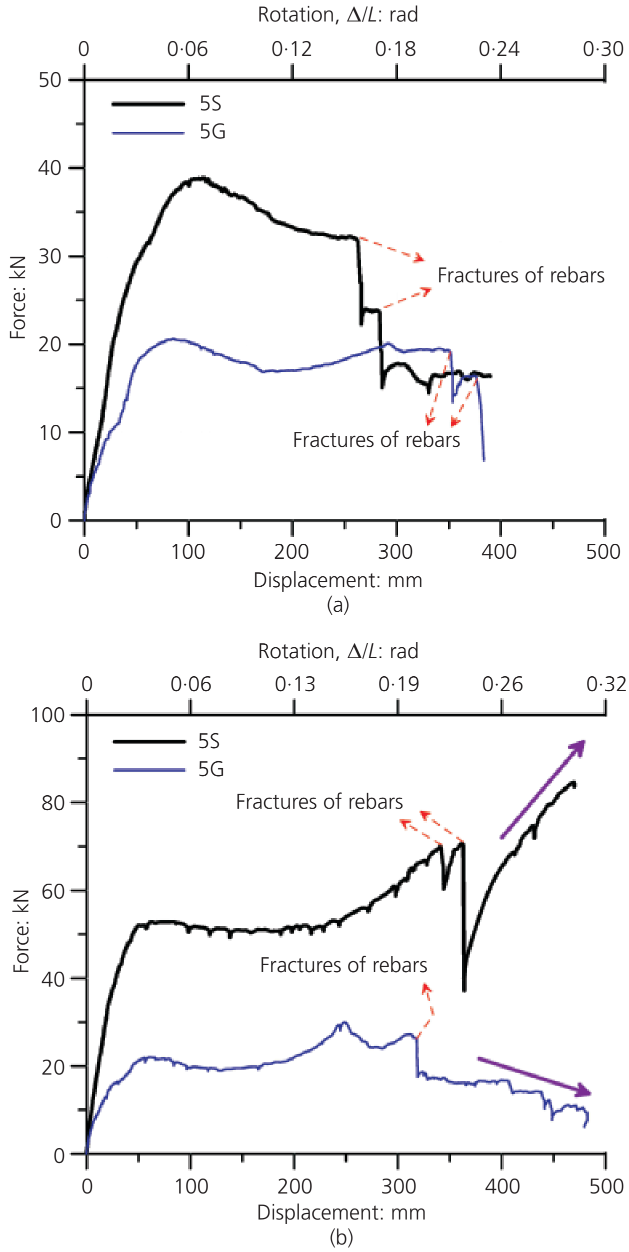

Figure 10. Load–displacement relationships of (a) sub-assemblage from five-storey structure and (b) sub-assemblage from eight-storey structure

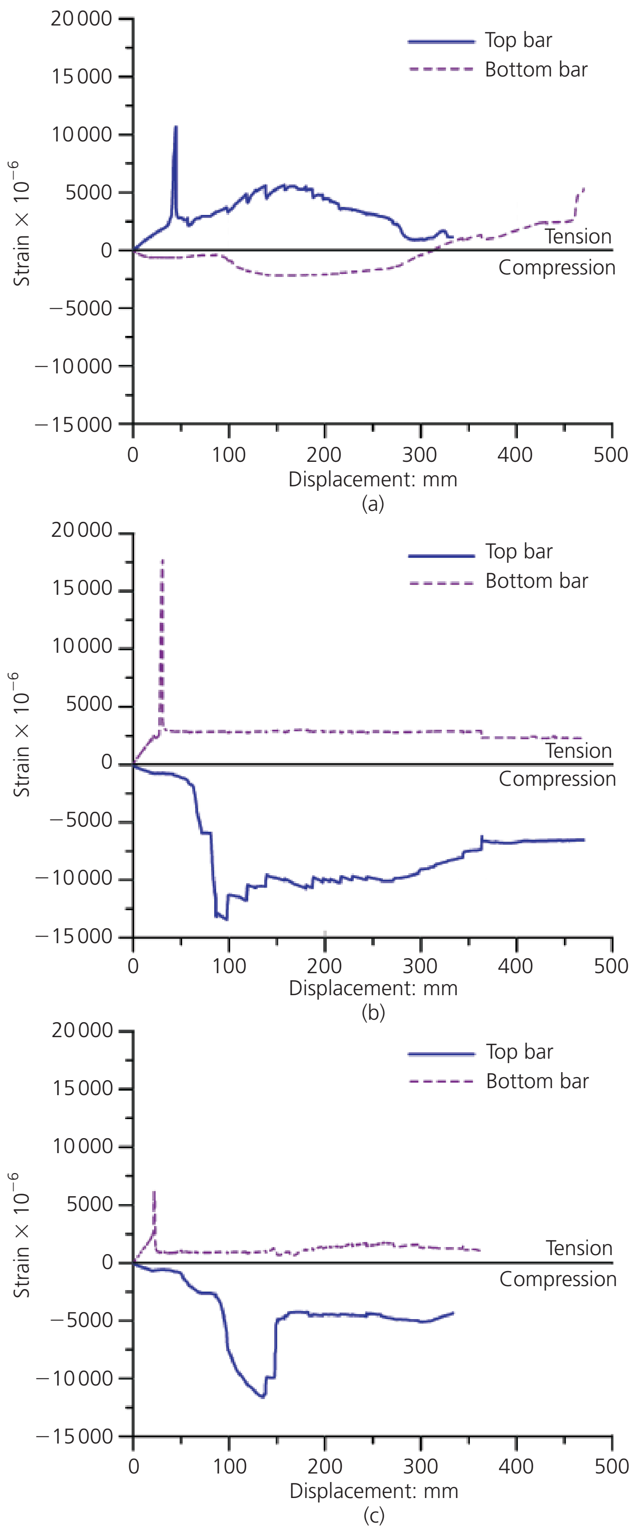

Figure 11. Strain of beam reinforcing steel in specimen 8S: (a) left end of left-hand beam (LL); (b) right end of left-hand beam (RL); (c) left end of right-hand beam (LR)

evaluated by pushdown analysis using the program code SAP2000 (CSI, 2004). The pushdown analysis was applied by gradually increasing the vertical displacement of the girder-removed column joint and computing element forces corresponding to the given deformation level to investigate the resistance of the structure against progressive collapse. Publications of the GSA (2003) and DoD (2005) proposed an amplification factor of 2 for static analysis to account for dynamic redistribution of forces. The load combination proposed by the GSA (2003) is

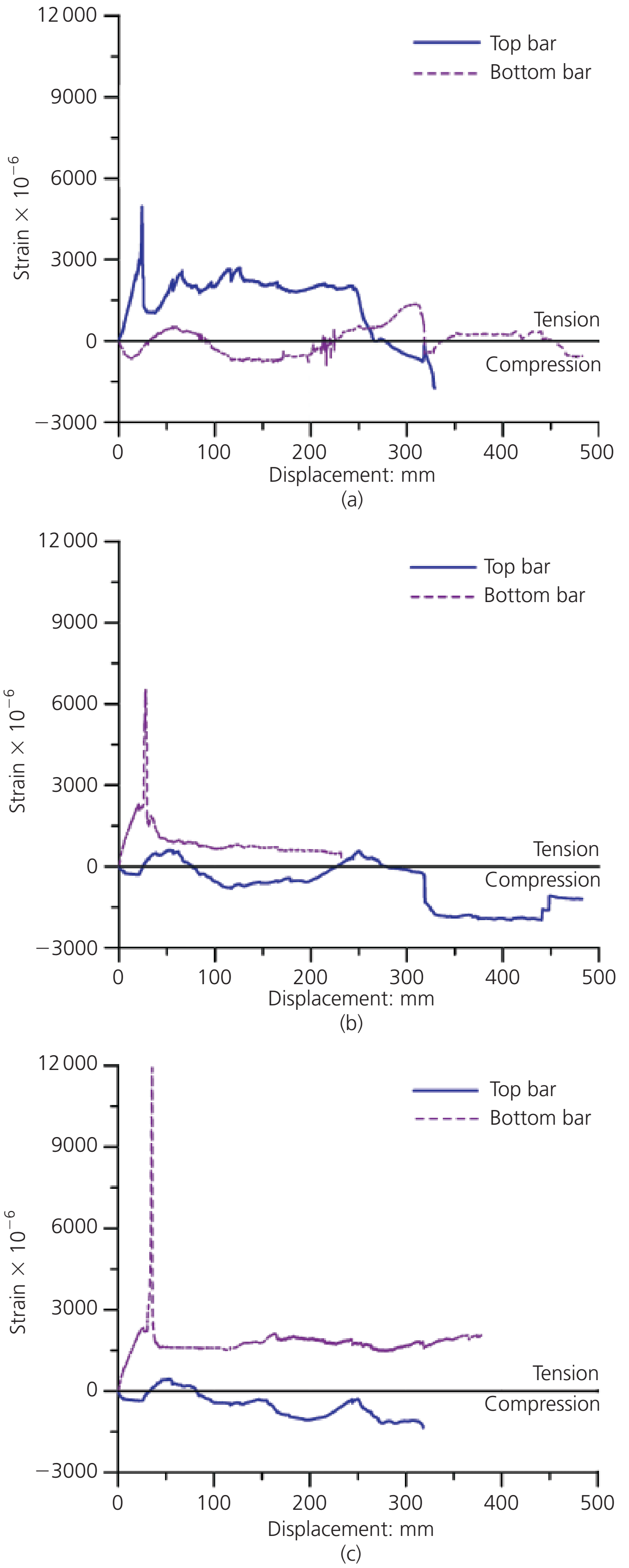

Figure 12. Strain of beam reinforcing steel in specimen 8G: (a) left end of left-hand beam (LL); (b) right end of left-hand beam (RL); (c) left end of right-hand beam (LR)

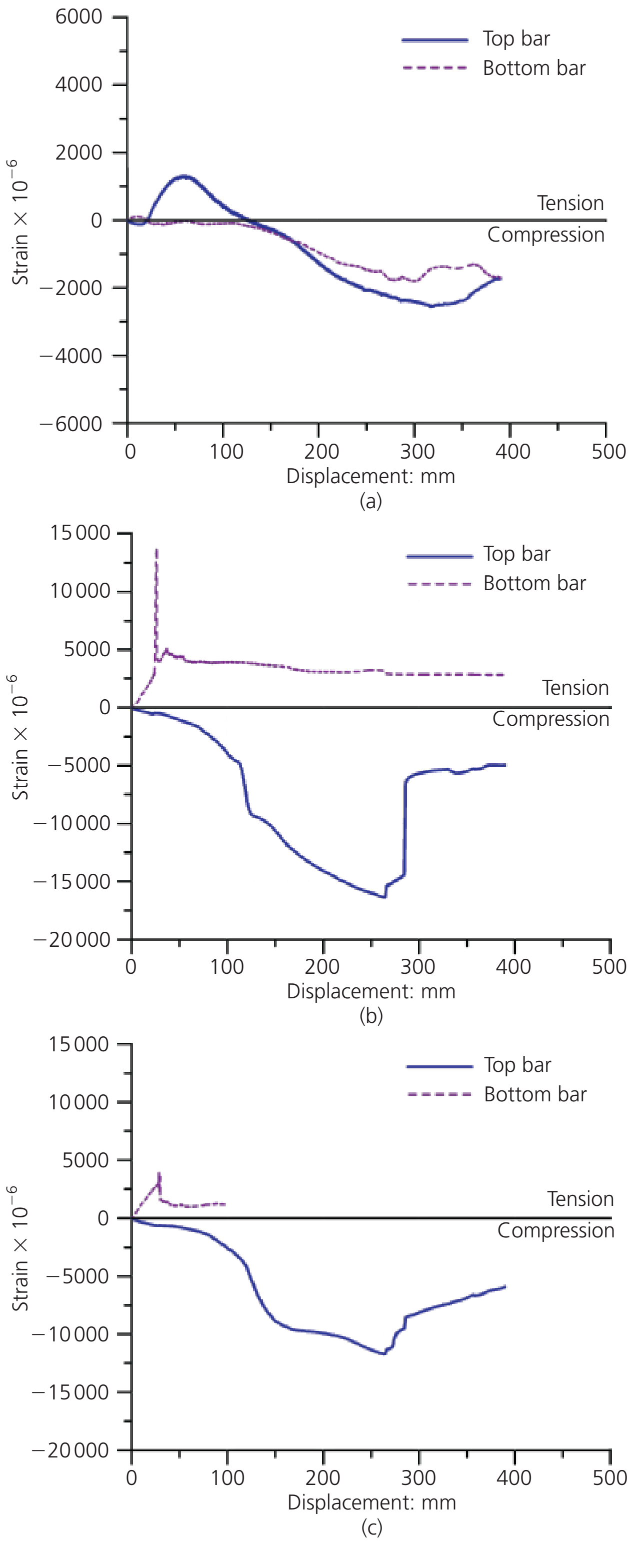

Figure 13. Strain of beam reinforcing steel in specimen 5S: (a) left end of left-hand beam (LL); (b) right end of left-hand beam (RL); (c) left end of right-hand beam (LR)

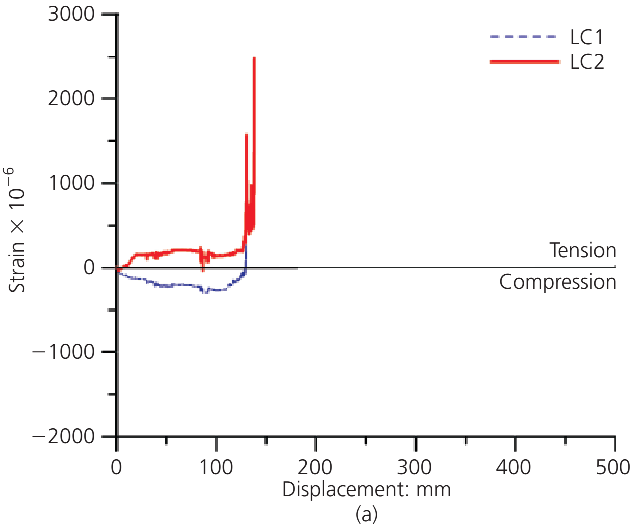

Figure. 14 Strain of exterior column reinforcing steel: (a) 8G; (b) 8S

$$2[\text{dead load} + (0{\cdot}25 \times \text{live load})]$$

and that of the DoD (2005) is

$$2[(1{\cdot}2 \times \text{dead load}) + (0{\cdot}5 \times \text{live load})] + 0{\cdot}2 \times \text{wind load}$$

In this study, the load combination of the GSA (2003) was selected for pushdown analysis. This amplified load was applied only in the spans in which a column was removed while unamplified load was applied in the other spans (Figure 15). If the maximum load factor from pushdown analysis is less than 1·0, the structure may not resist progressive collapse caused by loss of a column. The non-linear force–deformation relationship

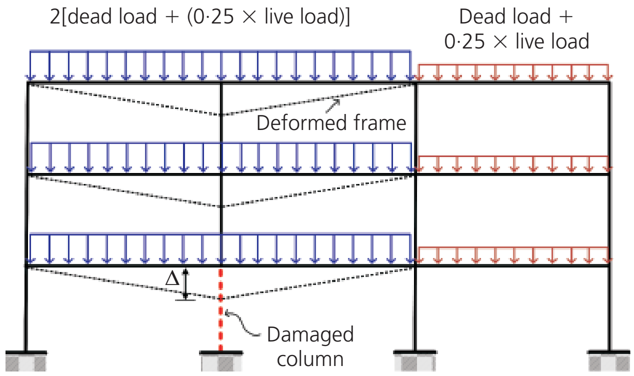

Figure 15. Applied gravity load for collapse analysis

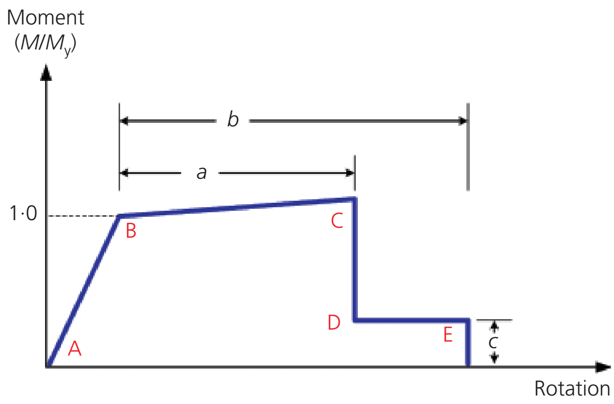

Figure 16. Plastic hinge model of beam elements

of structural members presented in FEMA-356 (FEMA, 2000) and depicted in Figure 16 was used in the pushdown analysis. The parameters a and b were determined to be 0·023 and 0·043 rad, respectively (based on Tables 6 and 7 of FEMA-356). The residual strength parameter c was assumed to be 0·2. The GSA guidelines recommend the value of 0·105 rad as an acceptance criterion for non-linear analysis of RC beams, which corresponds to approximately twice the limit state of the FEMA-356 non-linear model. The non-linear model shown in Figure 16 does not consider catenary action of members at large deformation. However, as observed in this study and in previous research (Kim and Yu, 2011; Sasani and Kropelnicki, 2008; Yi *et al.*, 2008), additional resistance to progressive collapse can be provided by catenary action in properly detailed RC frames.

The limit states for bending members proposed in FEMA-356 and used to produce the pushdown curve shown in Figure 17 were obtained from cyclic tests of members. However, it is considered that in the presence of repeated plastic cycling, the maximum deformation demand that an element or structure can accommodate during ground motion should be limited to about 50–60% of its ultimate deformation capacity attained under unidirectional loading (Panagiotakos and Fardis, 2001; Teran-Gilmore and Bahena-Arredondo, 2008). Therefore, to analyse structures using the member limit states recommended in FEMA-

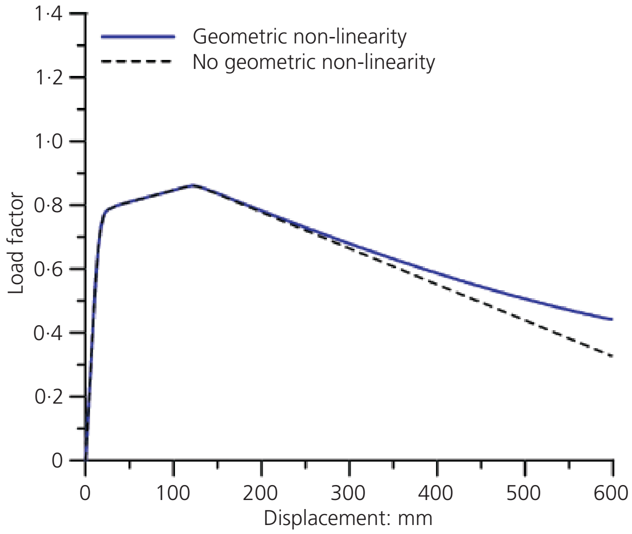

Figure 17. Pushdown curves of the eight-storey analysis model with and without considering geometric non-linearity

356 may underestimate their progressive collapse-resisting capacity. Therefore, in addition to the FEMA-recommended parameters for the non-linear force–deformation relationship, the values recommended in the GSA guidelines for RC beams and those determined based on the experimental results obtained in this study were also applied in the pushdown analysis and the results were compared. It can be observed in Figure 2(b) that when the pushdown curve starts to re-increase due to catenary action, the bending moment starts to decrease. In the pushdown curve of specimen 8S shown in Figure 10(b), this point corresponds to vertical displacement of approximately 250 mm. This displacement divided by the span length (1565 mm) results in beam rotation of 0·15 rad, which is a little larger than the GSA-recommended value of 0·105 rad.

Figure 17 shows the pushdown curves of the model structure obtained using the FEMA-recommended force–deformation relationship, with and without considering catenary action, with the first-storey second column from the left removed. The maximum strength is close to (but slightly less than) 1·0, which does not satisfy the safety criterion specified in the GSA guidelines. However, previous research (Kim *et al.*, 2009b) showed that structures with a maximum strength of less than 1·0 obtained from pushdown analysis might prove to have enough strength to resist progressive collapse through dynamic analysis, especially when the maximum strength is close to 1·0. In the case catenary action was not considered, the curve decreased more rapidly after maximum strength was reached. Figures 18 and 19 compare the distribution of axial force and bending moment of structural elements at a vertical displacement of 500 mm. When catenary action was not considered (Figure 18), collapse was resisted by the bending moments of the girders and axial forces of the columns. However, when catenary action was considered (Figure 19), the bending moments were reduced but axial forces of girders were significantly increased. This resulted in an increase of the pushdown curve.

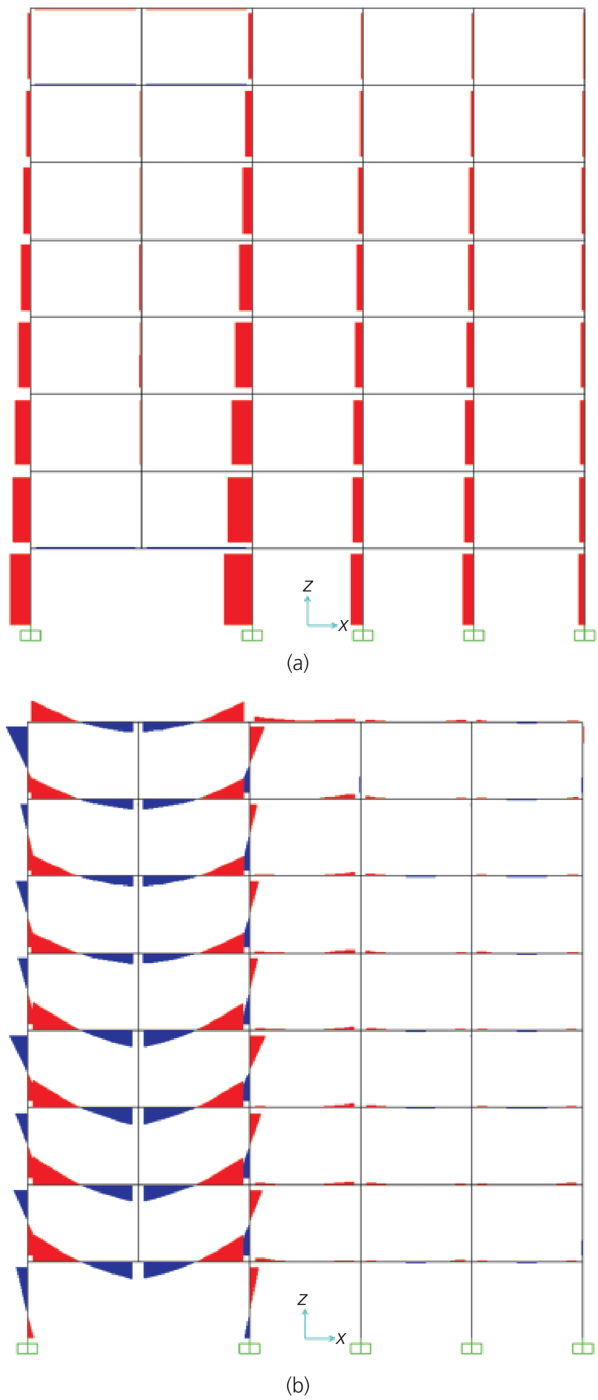

Figure 18. Member force at vertical displacement of 500 mm without considering catenary action: (a) axial force; (b) bending moment

Figure 20 compares the pushdown curves of the model structure obtained using the FEMA-356 non-linear force–deformation

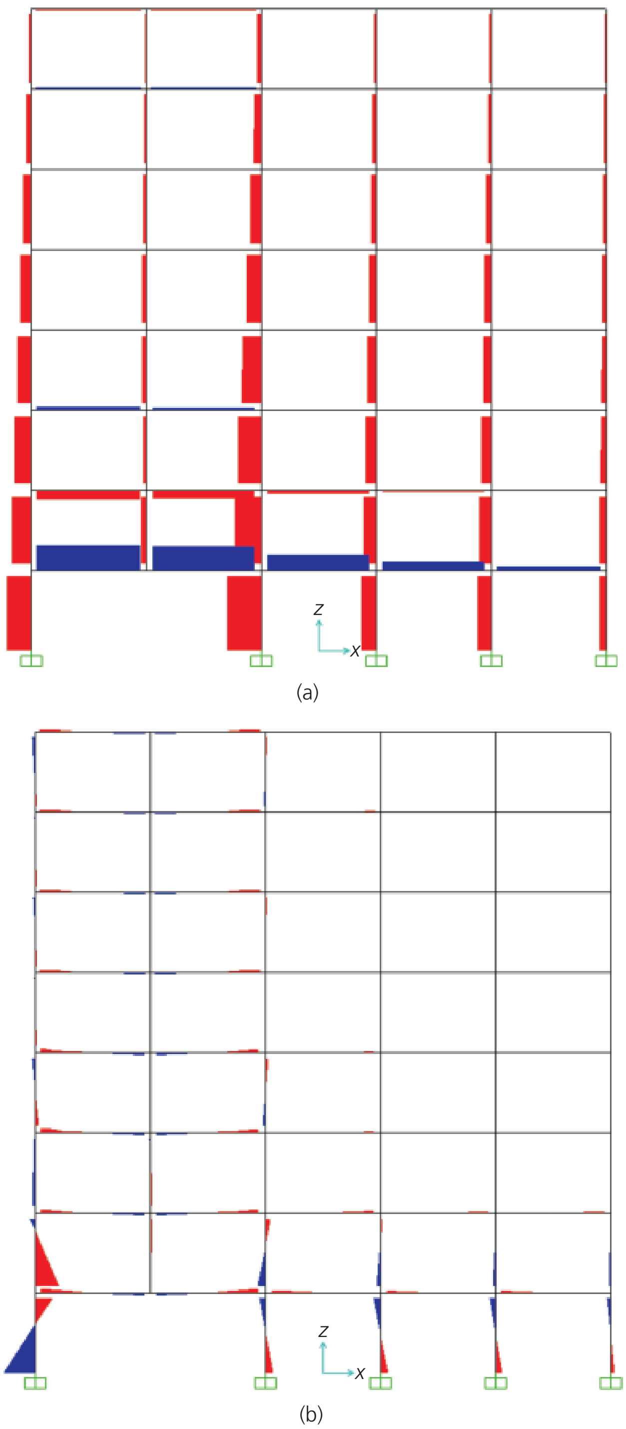

Figure 19. Member force at vertical displacement of 500 mm considering catenary action: (a) axial force; (b) bending moment

parameters and the parameters obtained from the experiment. When the FEMA-356 parameters were used, the pushdown curve started to decrease at a vertical displacement of approximately 130 mm. However, the pushdown curve obtained using the experimental force–displacement relationship kept increasing, similar to the experimental results of specimen 8S. When the

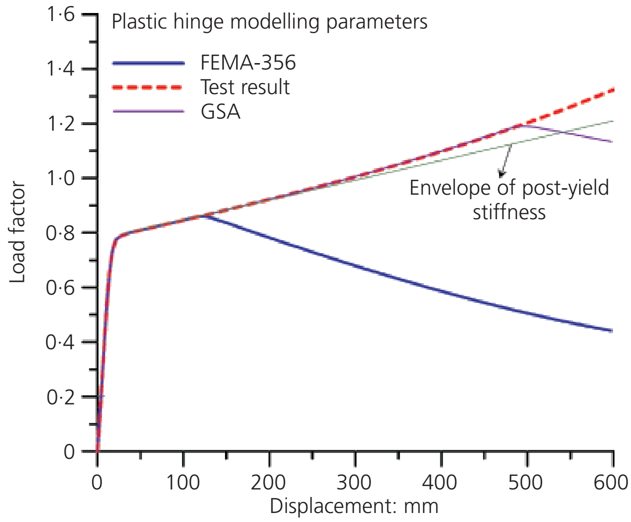

Figure 20. Pushdown curves of the beam–column sub-assemblage structure using different plastic hinge modelling parameters

GSA-recommended limit state was applied, the strength started to decrease at a vertical displacement of approximately 500 mm. Therefore, based on the limited test results obtained in this study, the limit states recommended in the GSA guidelines are considered to be more reasonable than the non-linear model based on FEMA-356 in defining the progressive collapse-resisting capacity of RC moment frames.

Conclusions

Experiments were carried out to investigate the progressive collapse-resisting capacity of RC beam–column sub-assemblages designed with and without seismic load. The two-span sub-assemblages were designed as part of five- and eight-storey RC moment-resisting frames. Based on the test results, the performance of an eight-storey RC moment frame with a missing column was evaluated by pushdown analysis and the results were compared with those obtained by using the limit states recommended in FEMA-356 and the GSA guidelines.

According to the experimental results, the force–displacement relationship of the specimen designed for seismic loading and having adequate concrete strength kept increasing even after fracture of the lower rebars due to the catenary action of the upper rebars. However, the non-seismically designed specimens (designed with wider-spaced stirrups/tie bars and with their lower beam longitudinal rebars not anchored by standard hooks) failed by pulling out of rebars and crushing of concrete at the exterior column–girder joint before catenary action was activated. The seismically designed specimen with low-strength concrete failed by joint failure before catenary action was activated. Based on the test results, it was concluded that RC moment-resisting buildings designed with seismic detailing might have significant resisting capacity against progressive collapse initiated by sudden loss of a column; non-seismically designed structures or seismically designed structures with deteriorated concrete strength might be vulnerable to progressive collapse. Finally, the non-linear pushdown analysis of the prototype structure showed that the limit states recommended in the GSA guidelines are more reasonable than the FEMA-356-based non-linear model for defining the progressive collapse-resisting capacity of RC moment frames.

Acknowledgement

This research was financially supported by the super-tall building R&D project of the Korean Ministry of Land, Transport, and Maritime Affairs (09CHUD-A053106-01-000000).

REFERENCES

ACI (American Concrete Institute) (2004) *ACI Committee 315 Detailing Manual*. ACI, Farmington Hills, MI, publication SP-66(04).

ACI (2005) *Committee 318 Building Code Requirements for Structural Concrete and Commentary.* ACI, Detroit, MI.

ASCE (American Society of Civil Engineers) (2005) ASCE7-05: Minimum design loads for buildings and other structures. ASCE, New York.

CEN (European Committee of Standardization) (2002) *Eurocode 1, Actions on Structures*. CEN, Brussels.

CSI (Computer and Structures, Inc.) (2004) *SAP2000, Structural Analysis Program*. CSI, Berkeley, CA.

DoD (Department of Defense) (2005) *Design of Buildings to Resist Progressive Collapse. Unified Facilities Criteria (UFC) 4-023-03*. DoD, Washington, DC.

Ellingwood BR (2006) Mitigating risk from abnormal loads and progressive collapse. *Journal of Performance of Constructed Facilities* **20(4)**: 315–323.

Ellingwood BR, Smilowitz R, Dusenberry DO, *et al.* (2007) *Best Practices for Reducing the Potential for Progressive Collapse in Buildings*. National Institute of Standards for Technology, Gaithersburg, MD, Report NISTIR 7396.

FEMA (Federal Emergency Management Agency) (2000) *Prestandard and Commentary for the Seismic Rehabilitation of Buildings*. FEMA, Washington, DC, Report FEMA-356.

GSA (General Services Administration) (2003) *Progressive Collapse Analysis and Design Guidelines for New Federal Office Buildings and Major Modernization Projects*. GSA, Washington, DC.

ICC (International Code Council) (2006) *International Building Code*. ICC, Falls Church, VA.

Khandelwal K and El-Tawil S (2005) Progressive collapse of moment resisting steel frame buildings. *Proceedings of the 2005 Structures Congress and the 2005 Forensic Engineering Symposium, New York*.

Kim H, Kim J and An D (2009a) Development of integrated system for progressive collapse analysis of building structures considering dynamic effects. *Advances in Engineering Software Archive* **40(1)**: 1–8.

Kim J and An D (2009) Evaluation of progressive collapse potential of steel moment frames considering catenary action. *The Structural Design of Tall and Special Buildings* **18(4)**: 455–465.

Kim J and Yu J (2011) Progressive collapse analysis of reinforced concrete moment frames considering geometric nonlinearity. *Magazine of Concrete Research*, in press.

Kim T and Kim J (2009) Collapse analysis of steel moment frames with various seismic connections. *Journal of Constructional Steel Research* **65(6)**: 1316–1322.

Kim T, Kim J and Park J (2009b) Investigation of progressive collapse-resisting capability of steel moment frames using push-down analysis. *Journal of Performance of Constructed Facilities* **23(5)**: 327–335.

Milner D, Gran J, Lawver D, *et al.* (2007) FLEX analysis and scaled testing for prediction of progressive collapse. *Proceedings of 1st International Workshop on Performance, Protection and Strengthening of Structures under Extreme Loading* (Protect 2007), *Whistler, Canada*.

Panagiotakos TB and Fardis MN (2001) Deformations of reinforced concrete members at yielding and ultimate. *ACI Structural Journal* **98(2)**: 135–148.

Sasani M and Kropelnicki J (2008) Progressive collapse analysis of an RC structure. *The Structural Design of Tall and Special Buildings* **17(4)**: 757–771.

Starossek U (2007) Typology of progressive collapse. *Engineering Structures* **29(9)**: 2302–2307.

Teran-Gilmore A and Bahena-Arredondo N (2008) Cumulative ductility spectra for seismic design of ductile structures subjected to long duration motions: concept and theoretical background. *Journal of Earthquake Engineering* **12(1)**: 152–172.

Tsai MH and Lin BH (2008) Investigation of progressive collapse resistance and inelastic response for an earthquake-resistant RC building subjected to column failure. *Engineering Structures* **30(12)**: 3619–3628.

Yi WJ, He QF, Xiao Y and Kunnath SK (2008) Experimental study on progressive collapse-resistant behavior of reinforced concrete frame structures. *ACI Structural Journal* **105(4)**: 433–439.

WHAT DO YOU THINK?

To discuss this paper, please submit up to 500 words to the editor at www.editorialmanager.com/macr by 1 October 2011. Your contribution will be forwarded to the author(s) for a reply and, if considered appropriate by the editorial panel, will be published as a discussion in a future issue of the journal.